JOURNAL OF MATERIALS SCIENCE 33 (1998) 659–667

Synthesis of (Pb,La) (Zr,Ti)O_3 films using a diol based sol–gel route

R. KURCHANIA, S. J. MILNE
Division of Ceramics, School of Materials, University of Leeds, Leeds LS2 9JT, UK

Morphotropic phase boundary compositions of lead zirconate titanate (PZT) modified with 2, 5 and 10 mol % lanthanum (PLZT) have been prepared using a diol based sol–gel route. Thin films of these PLZT compositions were fabricated on platinized silicon substrates by a spin coating technique. The effects of firing temperature and lanthanum modifications were investigated with regard to phase development, microstructure, and ferroelectric and dielectric characteristics. A strong ⟨1 1 1⟩ orientation developed as the amount of lanthanum doping increased. The results indicate that the values of remanent polarization, P_r, and dielectric constant, ε_r, decrease, relative to unmodified PZT, for films modified with 2 and 5 mol % lanthanum. The 5 mol % La films for example had a P_r of 14 $\mu C\,cm^{-2}$ and an ε_r value of 700 compared to 31 $\mu C\,cm^{-2}$ and 1480 for undoped PZT films. At these La concentrations there was also an improvement in the leakage current density by two orders of magnitude compared with unmodified PZT. The 10 mol % La sample did not exhibit any switchable polarization behaviour. © *1998 Chapman & Hall*

1. Introduction

The sol–gel processing of thin films of lead zirconate titanate (PZT) has received a considerable amount of attention in the last decade. It offers the potential for close control of the chemical composition and allows for low temperature processing conditions to be used [1–5]. Ferroelectric films of PZT and related compositions are of interest for the fabrication of novel functional devices, such as non-volatile memories, piezoelectric resonators, and pyroelectric detectors; La modified PZT (PLZT) is of special interest for incorporation in electro-optic devices [6–10]. There are of course other deposition processes that can be used to fabricate ferroelectric thin films; these include physical vapour deposition and metal-organic chemical vapour deposition techniques. However, it is arguably easier to control the composition and chemical homogeneity of multicomponent systems using sol–gel methods.

Sol–gel thin-film processing involves the synthesis of a gel-precursor solution, or sol, which is applied to a substrate using spin-on or dip-coating techniques; the resulting gel layer is then thermolysed to form a ceramic film. Generally, thermolysis is carried out in two stages, by employing a hot-plate prefiring step at lower temperature such as 300–400 °C, followed by a final firing treatment at 600–700 °C.

In the mid 1980's the first $PbTiO_3$ (PT), PZT and PLZT sol synthesis route was developed using a solution of lead acetate, and titanium and zirconium propoxides in a 2-methoxyethanol (MEO) solvent system [11]. This process has since found widespread acceptance and use. The zirconium and titanium propoxide starting reagents are very sensitive to moisture from the atmosphere and must be handled in dry atmosphere glove box conditions. In addition the sol synthesis reflux and distillation reactions must be performed using Schlenk 'vacuum' line techniques. The final stage in the synthesis reaction is to initiate a controlled partial hydrolysis of the Ti and Zr propoxide derivatives by deliberate additions of H_2O/alcohol mixtures to produce a polymeric type sol which can be used for thin film deposition. A variety of closely related routes have been developed based on the MEO system [12–14]. The limiting thickness for crack-free single layer films is usually about 0.1 μm for these PZT films [15]. Thicker single layers crack mainly as a result of the volume shrinkage on conversion of the low density gel layer to a crystalline film and because of the thermal expansion mismatch between film and substrate. Consequently a multiple-coating technique is required to build up films > 0.1 μm thick.

An alternative sol–gel route has been developed in which lead acetate and titanium and zirconium alkoxides are dissolved in acetic acid [3] and processed to form a coating sol. A crack-free layer on platinized silicon substrates can be made, up to a thickness of ~ 0.2 μm [16]. This route involves less complex chemical processing conditions than the MEO route as the reagents are ultrasonically mixed together in acetic acid and no reflux or distillation is required. A related acetate based sol–gel route has been used to prepare multilayer films up to a thickness of ~ 8.0 μm, using an automatic multiple coating technique [17–19] in which each layer was ~ 0.05 μm thick. The precursors used for the preparation of the PLZT films by this latter acetate route [17] are lead subacetate,

lanthanum acetate and an aqueous solution of zirconium acetate and titanium acetylacetonate.

In this laboratory we have developed another sol–gel process, in which dihydroxyalcohols (diols) are used as the solvent and gel-forming reagent. The chelating agent, acetylacetone, is used to modify the molecular structure of the titanium and zirconium propoxides so as to decrease their sensitivity towards hydrolysis. We have already demonstrated that PT and PZT films up to 1.0 μm thick can be made by this type of diol based sol–gel route from a single deposition and firing step [20–22], which indicates that the diol processing route yields a substantial improvement in the limiting thickness of crack-free films.

In this paper we report on developments to the diol route to enable the production of lanthanum modified PZT films.

2. Experimental procedures

The PLZT gel-precursor solutions were prepared according to the formula $Pb_{1-x}La_x(Zr_{0.53}Ti_{0.47})_{1-x/4}O_3$ with $x = 0$, 0.02, 0.05 and 0.1. The starting reagents for solution synthesis were lead acetate trihydrate $Pb(CH_3COO)_2.3H_2O$ (Aldrich Co., purity 99 + %), lanthanum acetate hydrate $La(CH_3COO)_3.xH_2O$ (Aldrich Co., purity 99.9%), titanium diisopropoxide bisacetylacetonate $Ti(OC_3H_7)_2(CH_3COCHCOCH_3)_2$, abbreviated as TIAA (Alfa Co., 75% in isopropanol), zirconium n-propoxide $Zr(OC_3H_7)_4$ (Alfa Co.), 1,3 propanediol $HO(CH_2)_3OH$ (Aldrich Co., purity 98%), and acetylacetone $CH_3COCH_2COCH_3$ (Aldrich Co., purity 99 + %). The lead and lanthanum acetates were dehydrated under reduced pressure (1×10^5 Pa) at 60 °C for 16 h. The zirconium n-propoxide was stabilized by refluxing with acetylacetone in a 1:2 molar ratio to promote the partial exchange of the n-propoxy groups by acetylacetonate groups. This zirconium complex, ZIAA, was then mixed with TIAA and 1,3 propanediol, in a ratio of 2 moles of diol per mol of (Zr + Ti). The mixture was heated under reflux conditions for 2 h. The dried lead and lanthanum acetates were mixed with 1,3 propanediol in a 1:3 molar ratio of (Pb + La) to diol, and then heated under reflux conditions for 2 h to form the lead and/or lead–lanthanum precursor sols. The two solutions were combined at ~80 °C. A further reflux for 5 h with one distillation after 2 h yielded the stock sol. The molarity was found by gravimetric analysis to be 1.12 M; n-propanol was used as the solvent to dilute the stock solution to 1 M for spin coating. In order to compensate for the lead losses during the heat treatment, 20 mol % excess lead was added at the beginning of the sol synthesis reaction. The solution synthesis procedure is shown schematically in Fig. 1. The viscosity of the PLZT sol was determined using Carri-Med Controlled Stressed Rheometer CSL 500 in the cone and plate measurement mode at room temperature.

The solutions were filtered through a 0.2 μm membrane filter before spin deposition at 1500 r.p.m. for 1 min onto 1 cm^2 $Pt/Ti/SiO_2/Si$ substrates. The

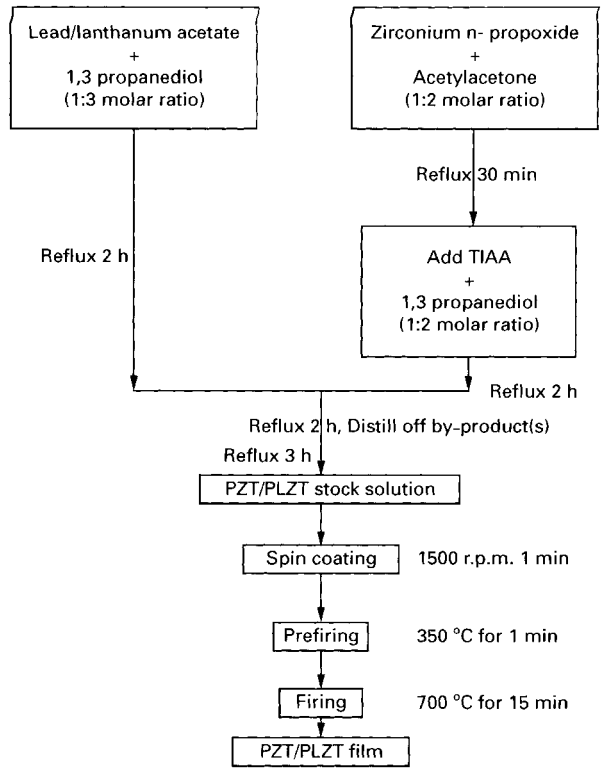

Figure 1 Flow diagram for the sol synthesis and film fabrication process for PZT and PLZT by the diol-based sol–gel route.

coated wet substrates were transferred to a hot plate for decomposition at 350 °C for 1 min and then fired at one of three different temperatures, 500, 600 or 700 °C, for 15 min in air. The samples were then inserted into a tube furnace held at the desired temperature and a thermocouple was placed alongside the sample in order to monitor both the heating rate and local firing temperature; the heating rate was typically found to be ~150 °C min^{-1}.

Thermogravimetric analysis (TGA) of the PZT and PLZT bulk gels was performed at a heating rate of 5 °C min^{-1} using a Stanton Redcroft TGA instrument. The gels to be analysed were prepared by heating the sols at 120 °C for 24 h. Phase analysis of the films was performed at room temperature by X-ray diffraction (XRD) techniques using a Philips APD 1700 diffractometer. Relative intensity peak height ratios were used to characterise the preferred orientation parameter α_{hkl}, e.g. $\alpha_{111} = I_{111}/(I_{100} + I_{110} + I_{111})$.

The surface morphology and cross-sections of the films were examined by scanning electron microscopy (SEM) using a Hitachi S-700 high resolution scanning electron microscope. Specimens were mounted on aluminium stubs using an epoxy adhesive. Carbon paint was applied to the specimen to provide a conductive path to the stub, and a sputtered gold surface coating prevented sample charging in the microscope.

For the measurement of electrical properties, capacitors were formed by sputtering 600 μm diameter gold electrodes onto the top surface of the films using a shadow masking method. A corner of the films was etched away using hydro-fluoroboric acid in order to reveal the bottom platinum electrode for

electrical contact to be made, so forming metal–oxide–metal (MOM) thin film capacitor configurations. The relative permittivity, ε_r, and dissipation factor, D, were measured using a Hewlett Packard 4192A impedance analyser at an applied field of 2 kV cm^{-1} and a frequency of 1 kHz. Ferroelectric hysteresis polarization–electric field characteristics were studied using a Radiant Technology RT-66A ferroelectric tester in the virtual ground mode at an applied field of 300 kV cm^{-1} and a frequency of ~60 Hz. Information on leakage current characteristics at a constant applied field of 50 kV cm^{-1} after a time interval of 30 min were studied using a Keithley 617 programmable electrometer.

3. Results

The use of propanediol and acetylacetonate chelating agents inhibited the hydrolysis and condensation of titanium and zirconium species [23, 24] and allowed stock sols to be produced which were stable against precipitation for at least 4 months when stored in air. In other experiments more concentrated $\geqslant$1.6 M sols precipitated after 4 h storage in air. The measured viscosity of the 1.0 M solutions used for coating purposes was ~2.0×10^{-2} Pa s.

The thermogravimetric analyses (TGA) revealed two distinct decomposition steps in the 0 and 2 mol % La samples, whereas in the two higher La contents, and especially the 10 mol % sample, a more continuous weight loss was observed, Fig. 2a. The thermal decomposition of dehydrated lanthanum acetate and lead acetate are shown in Fig. 2b; their contribution to the TGA trace of PLZT gels is discussed in the next section.

The effect of firing temperature on phase development of 2 mol % La doped PLZT films is shown in Fig. 3. The films fired at 500 and 600 °C for 15 min showed the presence of an intermediate pyrochlore structured phase, co-existing with a perovskite structured phase, whereas only the perovskite structured phase was observed in the 5 mol % lanthanum films fired at 700 °C for 15 min. Fig. 4 shows a comparison of the XRD patterns of films prepared from 0, 2, 5 and 10 mol % lanthanum, all fired at 700 °C for 15 min; the pyrochlore second phase was only evident in the 10 mol % sample.

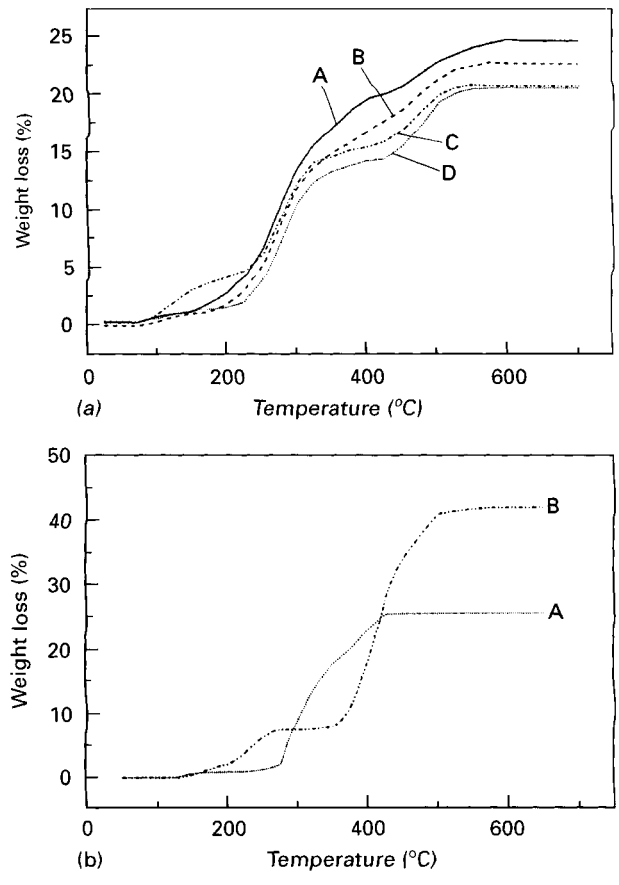

Figure 2 Thermogravimetric analysis curves for (a) dried PLZT sol with (A) 0, (B) 2, (C) 5 and (D) 10 mol % lanthanum, (b) (A) lead acetate and (B) lanthanum acetate.

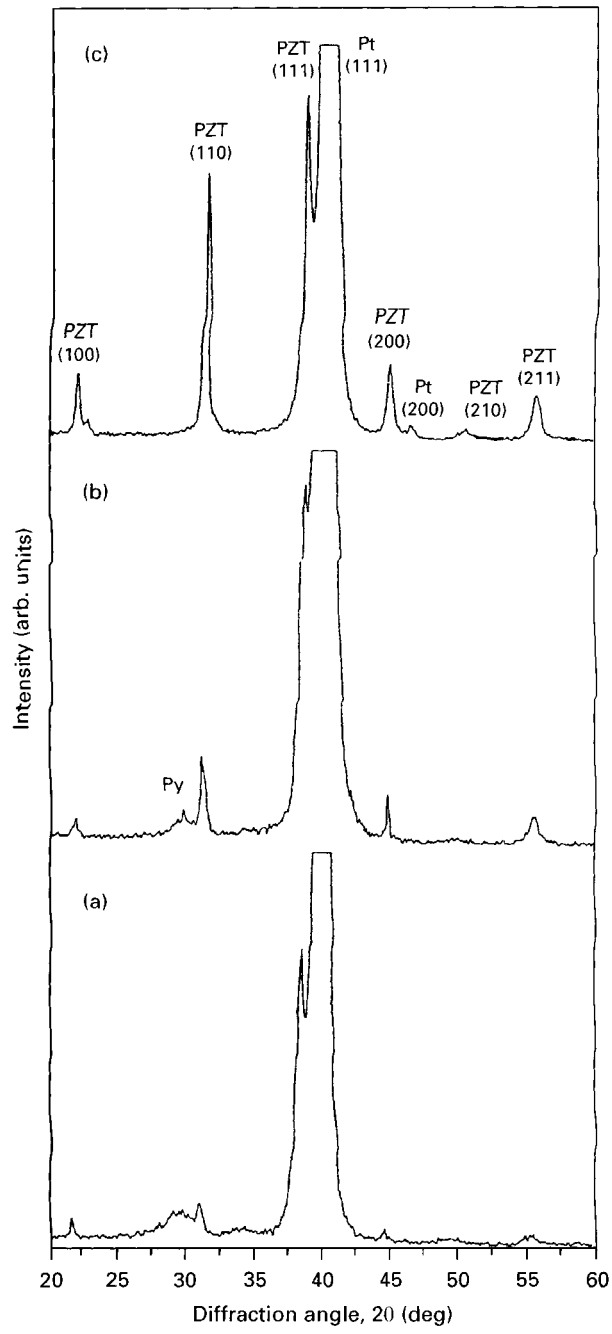

Figure 3 XRD pattern for the films doped with 2 mol % La, fired at (a) 500 °C, (b) 600 °C and (c) 700 °C.

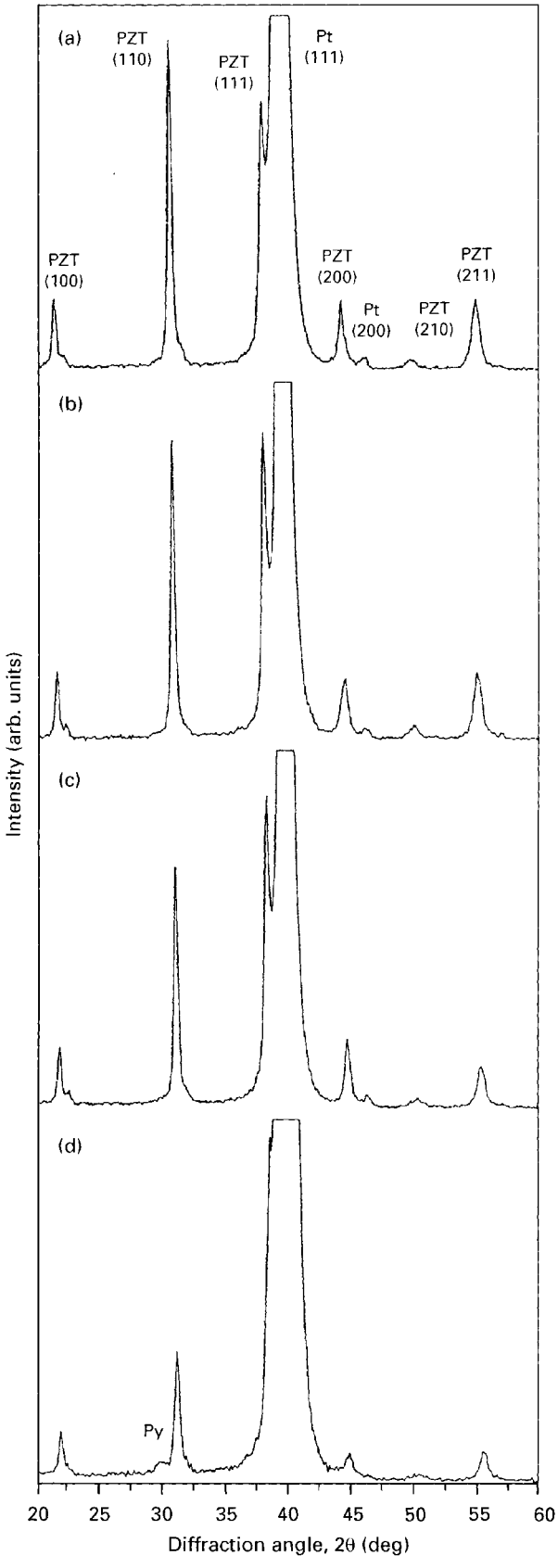

Figure 4 XRD pattern for the PLZT films fired at 700 °C for 15 min with (a) 0 mol %, (b) 2 mol %, (c) 5 mol % and (d) 10 mol % lanthanum.

This and other XRD data, summarized in Table I, shows that the amount of the pyrochlore structured second phase increased with increasing lanthanum concentration and, for a given composition, decreased with increasing firing temperature. An additional faint peak was observed at 22.6° 2θ, which is discussed later in the text.

Preferred orientation in the ⟨1 1 1⟩ direction was observed in all films. For films fired at 700 °C for 15 min, the XRD intensity ratio, $\alpha_{1\,1\,1}$, defined as $I_{1\,1\,1}/(I_{1\,0\,0} + I_{1\,1\,0} + I_{1\,1\,1})$, increased from 0.41 for films made from sols containing 0 mol % La to 0.77 for sols containing 10 mol % La. Correspondingly $\alpha_{1\,1\,0}$ decreased from 0.5 to 0.15 as shown in Table II but there was only a slight increase in $\alpha_{1\,0\,0}$.

An SEM cross-section of a 0.5 μm thick 5 mol % La film prepared by a single layer deposition is shown in Fig. 5. No cracks or other large scale surface defects were observed during optical microscopy studies but some isolated pit-marks, up to ~50 μm in diameter, were present. Subsequent work using less concentrated sols has shown that most of these features can be eliminated, but of course the single layer thickness was lower, ~0.25 μm, when these dilute, 0.5 M, sols were used. The surface microstructures of the 0, 2, 5 and 10 mol % lanthanum doped PZT samples fired at 700 °C are shown in Fig. 6(a–d). The 2, 5 and 10 mol % lanthanum content PLZT films had a fairly uniform microstructure with a grain size of ~0.1 μm. Undoped PZT films fired at 700 °C for 15 min showed a slightly different microstructure containing ~0.1 and 0.5 μm grains; texture in the larger grains suggested they were formed by the coalescence of smaller grains. The light areas in the 2 mol % La surface microstructure probably signify topographical variations, but there is a possibility that PbO on the surface of the films could, because of the high atomic number of Pb, contribute to contrast variations in these secondary electron micrographs. Analysis by energy dispersive spectroscopy (EDX-SEM Camscan series IV) was inconclusive due to the small grain size.

The effect of firing temperature on the polarization–electric field (P–E) response for the 2 mol % La doped PLZT films fired at 500, 600 and 700 °C is shown in Fig. 7. Firing at 500 °C did not result in any ferroelectric hysteresis response; hysteresis was observed at 600 °C but firing at 700 °C was required to produce well defined hysteresis loops. The ferroelectric and dielectric coefficients of the films fired at 600 and 700 °C are listed in Table III.

The P–E response of all film compositions fired at 700 °C is shown in Fig. 8; a summary of the measured electrical parameters is presented in Table IV. The 10 mol % La composition showed no evidence of ferroelectric switching and for the other compositions the remnant polarization (P_r) value decreased from 31 μC cm^{-2} for the 0 mol % La sample to 23 and 14 μC cm^{-2} for the 2 and 5 mol % La samples respectively. The coercive field values, E_c, of these two La samples were similar to one another and were some 50% higher than the 45 kV cm^{-1} value exhibited in the unmodified PZT films. The relative permittivities decreased from 1480 in PZT to 830 and 700 in the case of the 2 and 5 mol % La modified films. The dissipation factors (D) for single phase films were of the order of 3–4%. It was observed that the leakage currents decreased with increasing La additions; for example the incorporation of 5 mol % La produced

TABLE I Effect of La doping and firing temperature on phase development of PLZT films

Firing temp (°C)	Lanthanum content 0 mol %	2 mol %	5 mol %	10 mol %
700	Per	Per	Per	Per + Pyr
600	Per	Per + Pyr	Per + Pyr	Per + Pyr
500	Per + Pyr	Per + Pyr	Per + Pyr	Per + Pyr

Per = Perovskite phase; Pyr = Pyrochlore phase

TABLE II Effect of lanthanum doping on the preferred orientation parameter α_{hkl} for films fired at 700 °C for 15 min

La level (mol %)	α_{100}	α_{110}	α_{111}
0	0.07	0.50	0.41
2	0.08	0.44	0.46
5	0.09	0.27	0.64
10	0.12	0.15	0.77

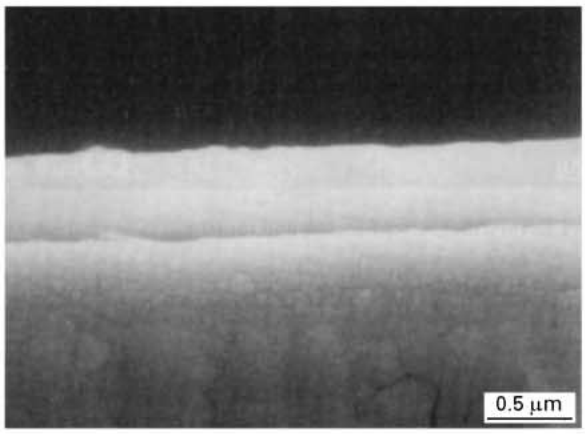

Figure 5 SEM cross-section of 0.5 μm thick PZT film modified with 5 mol % lanthanum.

a reduction from 2.0×10^{-7} to 3.0×10^{-9} A cm^{-2} in the value measured after 30 min.

4. Discussion

We have demonstrated that films of PLZT can be prepared successfully from a diol based sol–gel route. When lanthanum was introduced into the original synthesis scheme that had been previously developed for PZT films it was found that a slight precipitate formed in the sols [22, 25]. The cloudiness in the sols increased with increasing lanthanum levels; the precipitate is likely to be lanthanum acetate which is much less soluble than lead acetate in propanediol. Some changes to the synthesis conditions were consequently required in order to produce stable, precipitate-free precursor sols. The lead acetate and lanthanum acetate salts had to be dehydrated prior to use, whereas for PZT this was not necessary, and the Pb/La mixed precursor solution had to be diluted by increasing the diol to Pb/La ratio from 1 : 1 in the case of PZT to 3 : 1 for PLZT precursor sols.

In unmodified PZT gels there is a two-stage thermal decomposition with the second weight loss commencing at ~420 °C and ending at ~500 °C; the experimental TGA data for the lanthanum acetate starting reagent shows that its main decomposition (~30 wt %) occurs between ~375 and 500 °C, suggesting that the reason that the second weight loss in PLZT gels becomes less distinct with increasing levels of lanthanum is due to the combined decomposition of lanthanum acetate (or a closely related derivative formed during sol synthesis reflux reactions) and the base PZT-diol gel. This explanation implies that La does not enter the polymeric gel structure but instead unreacted lanthanum acetate exists in solution within the pore system of the polymeric (wet) gel network. In fact there is some debate as to whether or not lead is combined within the polymeric chains of PZT gels or is simply distributed as dissolved lead acetate. In previous work using nuclear magnetic resonance (NMR) spectroscopy we have shown that the main building block in the formation of polymeric gels in these diol systems is

$$\begin{bmatrix} AA\ \ AA \\ -M-O(CH_2)_3\ \ O-M- \\ AA\ \ AA \end{bmatrix}$$

where AA represents the bidentate CH_3COCH-$COCH_3$ ligand and M is Ti (or Zr) [26]. Further work is in progress to confirm the location of La and Pb in the gels.

Increases in the La levels in the films increased the minimum firing temperatures required to eliminate the additional pyrochlore phase identified by a broad peak centred at ~29.5° 2θ. Such a phase is often documented in the literature on lead zirconate titanate thin films and it is usually attributed to $Pb_2Ti_2O_6$ [27, 28] and $PbTi_3O_7$-type pyrochlore intermediates [29].

Transmission electron microscopy analysis has identified high levels of a pyrochlore phase in PbO-deficient surface layers of other PZT films [30]. The high surface area to volume ratio of submicron films, coupled to the relatively high vapour pressure of PbO at firing temperatures of 700 °C, makes PbO loss inevitable. It is also possible that chemical interactions with the bottom Pt/Ti electrode may consume Pb [28], so further depleting the Pb levels in the bulk of the ferroelectric film. It is thus common to add excess lead acetate to the starting sols or to apply a PbO gel precursor surface coating [28] to try to compensate for PbO losses. Often 10 mol % Pb is added to the

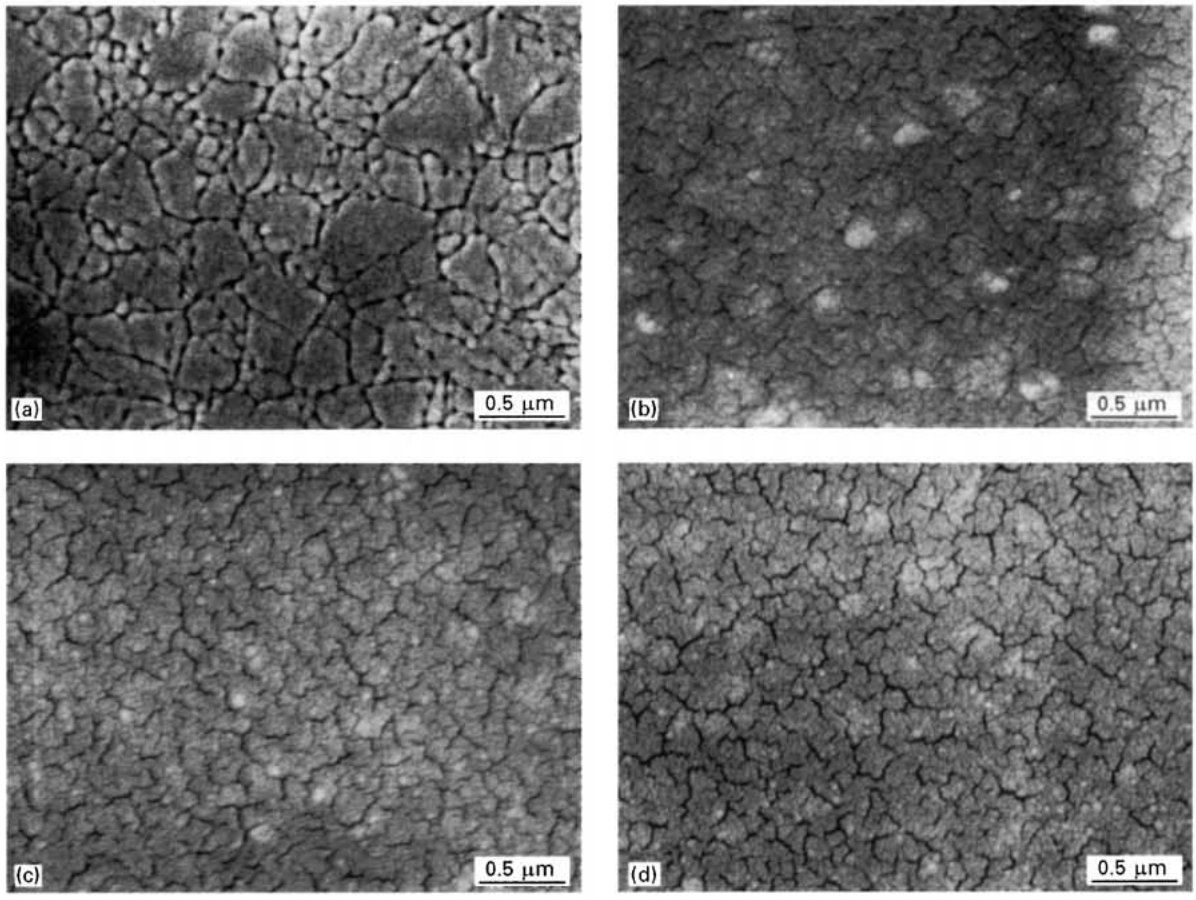

Figure 6 Microstructure of PLZT films fired at 700 °C for 15 min (a) 0 mol %, (b) 2 mol %, (c) 5 mol % and (d) 10 mol % lanthanum.

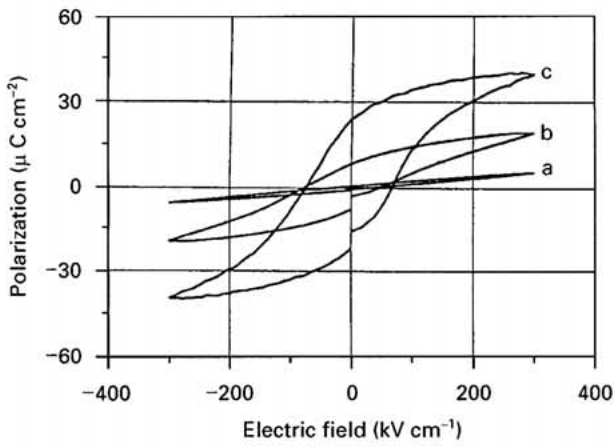

Figure 7 Ferroelectric hysteresis loop (P–E) for 2 mol % La doped PLZT films fired at (a) 500 °C, (b) 600 °C and (c) 700 °C for 15 min.

starting sols but in preliminary work on PLZT we found that an improved ferroelectric response resulted when the level of excess Pb was increased to 20 mol %. However even at this level it is quite possible that there is a slight Pb deficit at the film surface that promotes pyrochlore formation.

The increased presence of the pyrochlore structured phase in our higher La content samples may be an indirect compositional effect associated with a reduction in Pb to (Zr/Ti) ratio as the La level, x, increases in the $Pb_{1-x}La_x(Zr, Ti)O_3$ solid solutions. This argument assumes that La is not present in the intermediate phase(s), but transmission electron microscopy (TEM) compositional analysis of the second phase would be required before this could be confirmed. However, glancing angle XRD results in the literature show that the La_2O_3 and pyrochlore structured $PbTi_3O_7$ phases coexist near the surface of PLZT

TABLE III Effect of firing temperature on the ferroelectric and dielectric properties of 2 mol % La doped PLZT films

Firing Temp. (°C)	Remanent polarization P_r ($\mu C\,cm^{-2}$)	Coercive field E_c ($kV\,cm^{-1}$)	Relative permitivity ε_r	Dissipation factor D
700	23	70	830	0.04
600	8	60	425	0.05

TABLE IV Effect of lanthanum doping on electrical properties of films fired at 700 °C for 15 min

La level (mol %)	Remanent polarization P_r ($\mu C\,cm^{-2}$)	Coercive field E_c ($kV\,cm^{-1}$)	Relative permitivity ε_r	Dissipation factor D	Leakage current density J($A\,cm^{-2}$)
0	31	45	1480	0.03	2.0×10^{-7}
2	23	70	830	0.04	8.0×10^{-8}
5	14	66	700	0.04	3.0×10^{-9}
10	—	--	260	0.05	1.0×10^{-9}

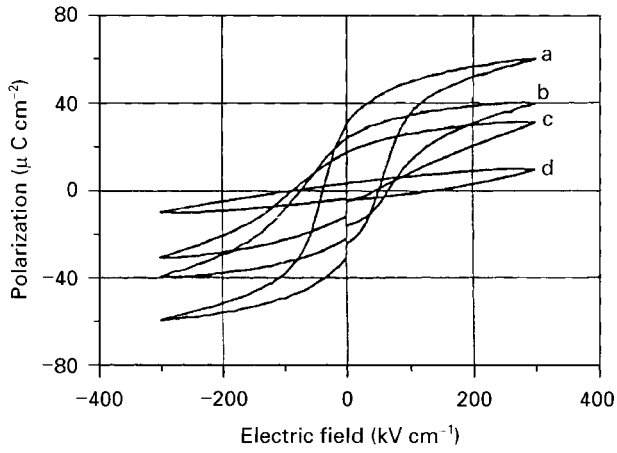

Figure 8 Ferroelectric hysteresis loop (P- E) for PLZT films fired at 700 °C for 15 min, doped with (a) 0 mol %, (b) 2 mol %, (c) 5 mol % and (d) 10 mol % lanthanum.

films [31], implying that La is not incorporated into the pyrochlore structured phase to any significant extent. Other workers have also noted the level of pyrochlore phase in PLZT thin films to depend on La levels [28], and in one case the pyrochlore structured phase was the only phase detected by X-ray diffraction for La compositions of 7 mol % and above [32].

A further possible compositional complication that may affect the pyrochlore stability is that Pb vacancies may actually be formed as charge compensators for donor dopants according to the formula $Pb_{1-3/2x}La_x(Zr, Ti)O_3$. Normally the B-site vacancy solid solution mechanism $Pb_{1-x}La_x(Zr, Ti)_{1-x/4}O_3$ is assumed, but it is quite possible that the alternative arises, especially in systems where processing conditions promote PbO volatilization. Compositional discrepancies that may affect pyrochlore formation and stability will clearly become greater as x increases.

The base $PbZr_{0.53}Ti_{0.47}O_3$ composition used in this study lies at the morphotropic phase boundary between rhombohedral and tetragonal phases. Reference to the PLZT equilibrium phase diagram [33] for bulk systems shows that La substitutions stabilize the tetragonal perovskite type phase for levels up to 12 mol % La, thereafter a cubic phase develops which is stable over the range of 12–15 mol % La. The X-ray diffraction patterns of our 0, 2, 5 and 10 mol % La film compositions can be indexed as being pseudocubic; this was probably due to peak broadening effects associated with stress in the films and/or the fine ~0.1 μm grain size. Consequently we assigned Miller indices on the basis of a pseudo-cubic symmetry system.

We have previously observed ⟨1 1 1⟩ preferred orientation in PZT films made using the diol sol–gel route [22]. The enhanced intensity of the (1 1 1) reflection found here for the PLZT films shows that an even greater level of ⟨1 1 1⟩ orientation occurs in PLZT films, with $\alpha_{1\,1\,1}$ increasing from 0.41 for undoped PZT films to 0.77 for 10 mol % La doped PZT films. In a separate experiment, *powders* of 0 and 5 mol % La doped PZT compositions were fired at 700 °C for 1 h and α parameters were calculated for these random powders. Using a comparable measurement method to that used for the PLZT thin films there was only a slight difference in α values between 0 and 5 mol % La powders with $\alpha_{1\,1\,1} = 0.12$ for 0 mol % La and 0.10 for 5 mol % La powders. Hence the observed increases in intensity of the (1 1 1) reflection with increasing La levels in the film samples are truly indicative of crystallite preferred orientation in the films, rather than to changes to the structure factor associated with La lattice substitutions.

The ⟨1 1 1⟩ PZT preferred orientation presumably originates from the ⟨1 1 1⟩ oriented Pt/Ti bottom electrode layer. There is a reasonably close lattice match between cubic Pt and PZT ($d_{1\,1\,1}$ Pt = 0.2265 nm [34], $d_{1\,1\,1}$ PZT (52/48) = 0.2351 nm [35]) which consequently would be expected to favour heterogeneous nucleation of ⟨1 1 1⟩ PZT. However Pt_3Ti-type and $PbPt_x$ ⟨1 1 1⟩ oriented phases [36, 37] are formed at the bottom electrode during firing; they also have lattice parameters close to that of PZT and so may also act as ⟨1 1 1⟩ PZT nucleation sites ($d_{1\,1\,1}Pt_3Ti = 0.2244$ nm [38], $d_{1\,1\,1}PbPt_x$ = 0.2340 nm (x = 5–7) [39]). A small diffraction peak at 22.6° 2θ is probably evidence of a Pt_3Ti phase [40], or closely related phase, in our samples. The JCPDS files indicate a (1 0 0) peak at 22.75° 2θ for Pt_3Ti, which is close to our extra peak. The reported $PbPt_x$, x = 5–7, phase [38, 39] has its (1 0 0) diffraction peak at 21.94° 2θ, signifying that this $PbPt_x$ composition range is not shown here, but possibly other similar phases could exist. This aspect requires further investigation.

Substitution of La^{3+} for Pb^{2+} decreased the measured pseudocubic lattice parameter with the measured $d_{1\,1\,1}$ value decreasing from 0.2351 nm for 0 mol % La to 0.2336 nm for 10 mol % La. From the published equilibrium phase diagram, as x increases the c/a ratio in the true tetragonal unit cell of PLZT, x/53/47, reduces until cubic symmetry occurs at the 12 mol % La composition [33]. In other words the enhanced ⟨1 1 1⟩ orientation for films with increasing La levels

is consistent with a reduction in the lattice spacing of the PLZT films approaching and more closely those of the ⟨1 1 1⟩ oriented phases, formed at the bottom electrode.

Moving on to the electrical properties of the films, the measured dielectric and ferroelectric parameters compare favourably with values reported in the literature [41, 42]. Information on this specific *x*/53/47 composition is however more limited than for zirconium-rich PLZT compositions, e.g. *x*/65/35, since the latter are of special interest for their electroptic applications. The *x*/53/47 PLZT composition was selected here since, as described previously in the text, the route was being developed from one first formulated for the popular 53/47 PZT composition.

Our films exhibited a strong dependence of the ferroelectric parameters on the firing temperature and on the incidence of additional non-ferroelectric pyrochlore structured phases. Values of the remanent polarization decreased with increasing La levels, possibly reflecting a reduction in the *c*/*a* ratio of the tetragonal unit cell for increasing La compositions, but the extent of ⟨1 1 1⟩ orientation in the films was also increasing with added La. As well as altering the orientation of polar axis with respect to the applied field during *P*–*E* hysteresis measurement, and consequently affecting measured polarization values, changing levels of ⟨1 1 1⟩ orientation could also in part signify varying stress levels in the films during crystallization which in turn would affect ferroelectric domain mobility and polarization values. This orientation effect will be investigated in more detail in future work.

Experimental current densities, *J*, were measured 30 min after applying the field; ideally *J* should first be measured as a function of time using an appropriate data acquisition system over a prolonged period to ensure that the current has decayed to a stable value for all compositions. Nevertheless it has been reported [41] that the leakage current measured 30 min after the voltage application accurately demonstrates the influence of composition on leakage current in donor doped PZT and so our data are of some relevance.

Our findings that La additions decreased the leakage current density by approximately two orders of magnitude is consistent with donor doping a p-type material such as PZT. When chemically pure PZT ceramics are fired in air, some PbO is lost due to volatilization; this coupled with reoxidation during high temperature processing leaves a net excess of lead vacancies and mobile positive holes ($Pb_{Pb} \rightarrow V''_{Pb} + 2h$), giving rise to p-type conductivity. Donor dopants such as La consequently decrease the leakage current due to electron–hole compensation mechanisms [29, 31, 41, 43].

5. Conclusions

The diol based sol–gel method can be modified to enable PLZT films up to 0.5 μm thick to be prepared by a single-layer deposition on platinized silicon substrates. Variations in La levels produced changes in the incidence of pyrochlore-type additional phases and in the levels of ⟨1 1 1⟩ preferred orientation. The 2 and 5 mol % films exhibited P_r values of 23 and 14 μC cm^{-2}, coercive fields of 70 and 66 kV cm^{-1} and relative permittivities of 830 and 700 respectively. For the highest La concentration studied, 10 mol %, it was not possible to prepare a single phase perovskite film even after firing at 700 °C. Consequently this 10 mol % PLZT composition exhibited inferior dielectric and ferroelectric coefficients.

Acknowledgements

Rajnish Kurchania is grateful to the ORS Awards Scheme and Tetley Lupton Scholarships for financial assistance. Technical discussions with Dr. Y. L. Tu, Dr. N. J. Ali and Mr. R. Holt are also gratefully acknowledged.

References

1. C. E. LAND, *J. Amer. Ceram. Soc.* **71** (1988) 905.
2. R. W. VEST and J. WU, *Ferroelectrics* **93** (1989) 21.
3. G. YI, Z. WU and M. SAYER, *J. Appl. Phys.* **64** (1988) 2717.
4. P. J. BORRELLI, P. H. BALLENTINE and A. M. KADIN, in *Mater. Res. Soc. Symp. Proc.* Vol. **243** (Materials Research Society, Pittsburgh, PA, 1992) p. 417.
5. C.H. PENG, J. CHANG and S. B. DESU, *ibid.* p. 21.
6. L. M. SHEPPARD, *Ceram. Bull.* **71** (1992) 85.
7. P. F. BAUDE, C. YE, T. TAMAGAWA and D. L. POLLA, in *Mater. Res. Soc. Symp. Proc.* Vol. **243** (Materials Research Society, Pittsburgh, PA, 1992) p. 275.
8. C. A. PAZ DE ARAUJO, L. D. McMILLAN and B. M. MELNICK, *Ferroelectrics* **104** (1990) 241.
9. T. KAWAGUCHI, H. ADACHI and K. SETSUNE, *Appl. Opt.* **23** (1984) 2187.
10. A. B. WENGER, S. R. J. BRUECK and A. Y. WU, *Ferroelectrics* **116** (1991) 195.
11. K. D. BUDD, S. K. DEY and D. A. PAYNE, *Brit. Ceram. Proc.* **36** (1985) 107.
12. K. C. CHEN, A. JANAH and J. D. MACKENZIE, in "Better ceramics through chemistry II", edited by C. J. Brinker, D. E. Clark and D. R. Ulrich, *Mater. Res. Soc. Symp. Proc.* Vol. **73** (Materials Research Society, Pittsburgh, PA, 1986) p. 731.
13. N. TOHGE, S. TAKAHASHI and T. MINAMI, *J. Amer. Ceram. Soc.* **74** (1991) 67.
14. Y. TAKAHASHI, Y. MATSUOKA, K. YAMAGUCHI, M. MUTSUKI and K. KOBAYASHI, *J. Mater. Sci.* **25** (1990) 3960.
15. S. H. PYKE, PhD thesis, University of Leeds, Leeds (1990).
16. C. K. KWOK, S. B. DESU and D. P. VIJAY, *Ferroelectrics Lett.* **16** (1993) 143.
17. G. H. HAERTLING, *Ferroelectrics* **116** (1991) 51.
18. *Idem., Integrated Ferroelectrics* **3** (1993) 207.
19. *Idem., Am. Ceram. Soc. Bull.* **73** (1994) 68.
20. N. J. PHILIPS, M. L. CALZADA and S. J. MILNE, *J. Non-Cryst. Solids* **147/148** (1992) 285.
21. M. L. CALZADA and S. J. MILNE, *J. Mater. Sci. Lett.* **12** (1993) 1221.
22. Y. L. TU and S. J. MILNE, *J. Mater. Sci.* **30** (1995) 2507.
23. M. GUGLIEMI and G. CARTURAN, *J. Non-Cryst. Solids* **100** (1988) 16.
24. S. A. MYERS and L. N. CHAPIN, *Mater. Res. Soc. Symp. Proc.* Vol. 200 (Materials Research Society, Pittsburgh PA, 1990) p. 231.
25. N. J. ALI, P. CLEM and S. J. MILNE, *J. Mater. Sci. Lett.* **14** (1995) 837.
26. N. J. PHILLIPS, S. J. MILNE, N. J. ALI and J. D. KENNEDY, *ibid.* **13** (1994) 1535,
27. M. V. RAYMOND, J. CHEN and D. M. SMYTH, *Integrated Ferroelectrics* **5** (1994) 73.
28. T. TANI and D. A. PAYNE, *J. Amer. Ceram. Soc.* **77** (1994) 1242.

29. M. V. RAYMOND and D. M. SMYTH, *Integrated Ferroelectrics* **4** (1994) 145.
30. K. G. BROOKS, I. M. REANEY, R. KLISSURSKA, Y. HUANG, L. BURSIL and N. SETTER, *J. Mater. Res.* **9** (1994) 2540.
31. C. SUDHAMA, J. KIM, J. LEE and V. CHIKARMANE, *J. Vac. Sci. Technol. B* **11** (1993) 1302.
32. G. TEOWEE, *Integrated Ferroelectrics* **4** (1994) 231.
33. G. H. HAERTLING and C. E. LAND, *J. Amer. Ceram. Soc.* **54** (1971) 1.
34. Powder Diffraction File, Card No. 4 802, (Joint Committee on Powder Diffraction Standards, Swarthmore, PA, 1979).
35. *Ibid.*, Card No. 33–784, (Joint Committee on Powder Diffraction Standards, Swarthmore, PA, 1979).
36. S.-Y. CHEN and I.-W. CHEN, *J. Amer. Ceram. Soc.* **77** (1994) 2332.
37. J. O. OLOWOLAFE, R. E. JONES Jr., A. C. CAMPBELL, R. I. HEDGE and C. J. MOGAB, *J. Appl. Phys.* **73** (1993) 1764.
38. Powder Diffraction File, Card No. 17–64, (Joint Committee on Powder Diffraction Standards, Swarthmore, PA, 1979).
39. *Ibid.*, Card No. 6–574, (Joint Committee on Powder Diffraction Standards, Swarthmore, PA, 1979).
40. Y. L. TU and S. J. MILNE, *J. Mater. Res.* **11** (1996) 2556.
41. D. DIMOS, R. W. SCHWARTZ and S. J. LOCKWOOD, *J. Amer. Ceram. Soc.* **77** (1994) 3000.
42. J. F. CHANG and S. B. DESU, *J. Mater. Res.* **9** (1994) 955.
43. R. GREEN and H. HAFFE, *J. Phys. Chem. Solids* **24** (1963) 979.

Received 3 February
and accepted 4 August 1997